3-(Aminopropyl)triethoxysilane modified CuO nanoparticles-mediated adsorbent for removal of methylene blue through polymer inclusion membranes transport: optimization of operational variables

Kiran Mustafa[a,b], Sara Musaddiq[a,*], Sarrah Farrukh[c], Sajjad Ahmad[d], Hifsa Rasheed[d], Imama Fayyaz[a]

[a]*Department of Chemistry, The Women University Multan, 66000, Pakistan, emails: drsara.chem@wum.edu.pk (S. Musaddiq), kiranmustafa100@gmail.com (K. Mustafa), imamafayyaz56@gmail.com (I. Fayyaz)*
[b]*Govt. Graduate College for Women Near GPO Khanewal, Higher Education Department Punjab Pakistan*
[c]*School of Chemical and Materials Engineering, National University of Science and Technology Islamabad, Pakistan, email: sarah.farrukh@scme.nust.edu.pk*
[d]*Pakistan Council of Research in Water Resources, Ministry of Science and Technology, Islamabad, Pakistan, emails: chsajjadahmad@hotmail.com (S. Ahmad), pcrwr2005@yahoo.com (H. Rasheed)*

ABSTRACT

The current study presents the fabrication of 3-(aminopropyl)triethoxysilane (APTES) enhanced CuO nanoparticles integrated polymer inclusion membranes (PIMs) and their application in the removal of the textile dyes via transportation from one phase to another. The said membranes were fabricated with facile diffusion induced phase inversion technique and were characterized with Fourier transform infrared spectroscopy and scanning electron microscopy. Later the membranes were employed in the self-made detachable cell with two compartments of glass and a steel clamp. The cell allows the installation of the PIM between the glass compartments, which is used for the transportation of the dye (methylene blue) from the feed phase to the strip phase. Different parameters, which can affect the transportation of the dye such as the pH of the feed and the acceptor phase, stirring speed, time, percentage of the carrier in the membrane and the concentration of the dye were optimized. After optimization, 97% transportation efficiency was achieved. In the study, the comparative analysis between the transportation of the dye by CuO nanoparticles integrated membranes and the 3-(aminopropyl)triethoxysilane modified CuO nanoparticles integrated membranes have also been conducted. The results of the comparative permeation study showed better transportation of the dye with the 3-(aminopropyl)triethoxysilane modified CuO nanoparticles integrated membranes.

Keywords: Nanoparticles; Membrane separations; Dyes; Transport; Water treatment

1. Introduction

Water scarcity is one of the major issues faced by the modern world. A broad range of pollutants such as pesticides [1], transition metals [2], organic compounds [3], endocrine disruptors [4] are responsible for polluting the already limited resources of freshwater. One of the major contributors to water pollutions is textile waste. It contains several toxic compounds including dyes [5]. Although dyes are attractive molecular species and few of their crystals

* Corresponding author.

are enough for apparent colors in solutions. They are integral part of the textile as well as paper, rubber, plastic, food and cosmetic industries. Despite of their remarkable uses, dyes are difficult to degrade biologically. They are available in diverse chemical structures and most of them have complex aromatic moieties. Moreover, it is quite hard to remove dyes even their fractions after decomposition remains toxic and harmful. A huge data is already published concerning the adverse health effects of dyes on humans, children and marine life. Mainly dyes are mutagenic and carcinogenic in humans. Furthermore, common diseases associated with dyes are allergy, abdominal pain, chromosomal damage, thyroid ailments and chromosomal damage. Before releasing to the environment, the dye waste of the industries is diluted to certain amounts, however, the dilution is not enough, and the waste is still hazardous to the environment. In addition to this, dyes form a layer over the water bodies hence preventing the sunlight to enter and thereby affecting the photosynthetic reaction [6].

Consequently, dyes remediation from wastewater before their discharge into the environment is mandatory. Therefore, several methods have been developed for treating textile waste. These include supramolecular mechanism, sequestering, [7,8] coagulations, electrochemical precipitation, nanofiltration, liquid–liquid extraction, adsorption, ionic liquid grafted magnetic nanoparticles, oxidation–ozonation and colloidal gas aprons (CGA) method is used for the removal of dyes as well [9–14]. Although these methods are supportive for dyes removal, tedious handling and treatment process restrict their use in a wide spectrum [15]. In a comparatively novel approach "polymer inclusion membranes (PIMs) are used for the eradication of the dyes. The PIMs are the type of liquid membranes and are fabricated by casting the solution containing polymeric matrix volatile solvent and plasticizer. After casting the solvent is evaporated resulting in the formation of the flexible, thin, stable and self-supporting membrane. These membranes are better than supported liquid membranes, in terms of enhanced stability, versatility and smaller loss of the carrier and ease of operation [16]. The membranes are widely employed for the extraction of a variety of metals ions from the feed solution [17,18]. This extraction ability of the PIMs has also been employed for the removal of the varying dyes by integrating the suitable material in them [19].

Despite the various application of PIMs in analytical chemistry, they are normally prepared by two major polymers, that is, cellulose triacetate (CTA) and polyvinyl chloride (PVC) [20]. The polymer is usually selected according to the required application. Sometimes a plasticizer is also added for the fabrication of these membranes for increasing the flexibility [21]. CTA has excellent salt rejection properties along with remarkable toughness, defiance to hydrolysis, resistance to biofouling, strength and adaptability. CTA is utilized in the fabrication of a variety of membranes such as composite membranes, Loeb-type blend and hollow fibers. CTA has proven to be extremely useful for the fabrication of this membrane due to the finite solubility, high flux and salt rejection [22]. Common methods for developing the CTA membranes are grafting, coating and blending. The surface modification method of the CTA membranes through grafting comprehends the formation of covalent

bonds between the CTA matrix and hydrophilic monomers by radiation, plasma, photochemical and chemical initiation. For the introduction of nanomaterials in the membranes, several techniques like sol-gel processes, thin film deposition, coating (interfacial polymerization, dip coating and layer-by-layer coatings), phase inversion, etc. have been used. The hydrophilic monomers that are most generally used for grafting are polybutylacrylate, polymethylacrylate and acrylic acid monomer [23]. In coating, evaporation and contact processes are used to coat a thin layer of hydrophilic polymers on the surface of CTA membranes. Hydrophilic CTA membranes can be easily synthesized by immersing the membranes in polyamide solution [24]. Contrary to post-fabrication procedures like coating and grafting, blending is "in process" moderation of the membranes [25].

As far as the transport mechanism of the PIMs is concerned, the details are not completely understood [16]. However, they generally establish the assumption is that: first, an analyte (such as a dye molecule) is extracted and forms an ion-pair with the carrier (such as modified nanoparticles) at the membrane/feed interface, followed by the subsequent diffusion of the ion pair into the strip phase. The chemical selectivity of the membranes is directly associated with the extraction constant whereas the rate of transport is influenced by the diffusion coefficient [26]. In some studies, it is suggested that the carriers have very restrained mobility within the matrix of the PIM, and the analyte must jump from carrier to carrier for crossing the membrane [27,28]. Hence it can be concluded that the transportation ability of the PIMs is associated with the integrated materials (carriers). The nature of the material is dependent on the type of application expected from the said membrane. Nowadays blending of inorganic oxide nanoparticles like nanoporous $CaCl_2$, hydroxyapatite/BN nanocomposites, $MnCO_3$ has been given much attention owing to the remarkable properties that they induce in the membranes, such as reduced fouling, flux enhancement, improved strength, dyes and other pollutant transportation, etc. [29–31]. CuO nanoparticles (CuO-np) have also been integrated into the membranes for improved performance of polymeric membranes, they can also be employed as the carriers in the membranes [32]. The amino group functionalized CuO-np has been found to be more compatible with the organic phase of the membrane matrix. The amino-modified CuO-np integrated membranes also depict improved hydrophilicity [33]. The amino groups can be added to the CuO-np via different chemicals, 3-(aminopropyl)triethoxysilane (APTES) serves the purposes efficiently, as a single pot reaction is enough for the synthesis of amino-modified nanoparticles [33]. In this study, APTES is used for the amino modification of the CuO nanoparticles.

Krishnamurthy et al. [34] have fabricated, copper(I) oxide (Cu_2O) nanoparticles integrated PES mixed-matrix membranes via phase inversion. The membrane performance was improved by the usage of Cu_2O nanoparticles in 1.5 wt.%. In another study conducted by Nasrollahi et al. [35], CuO-np was used in the polymeric matrix of the membranes and the membranes depicted promising anti-biofouling activity.

The polymeric membranes with no integrated material are not capable of transporting the materials from one phase or another. Because the integrated material functions

as the carrier and gets bound with the analyte at the membrane/feed phase interface. The difference in pH or some other parameter is responsible for the removal of the analyte at the membrane/strip phase interface. Transportation is driven by the chemical force [19]. In this study phase inversion method was used for the synthesis of CTA/CuO-np and CTA/A-CuO-np (ATPES) enhanced CuO-np) membranes. The prepared membranes were characterized with a scanning electron microscope (SEM) and Fourier transform infrared spectroscopy (FTIR). Dye transport experiments with an aqueous solution of methylene blue [28] were performed by employing the fabricated membranes.

2. Experimental

CuO-np was prepared by the procedure reported by Phiwdang et al. [36]. For that purpose, $Cu(NO_3)_2·3H_2O$ and copper chloride $CuCl_2$ were obtained from Sigma-Aldrich Chemicals, USA. The solutions of the precursors were made in deionized (DI) water. Afterwards dilute NaOH solution was added to obtain the alkaline environment. Black precipitates of the product were obtained and were washed repeatedly with DI water and absolute ethanol until neutral pH was obtained. Later, the product was dried at 80°C for 16 h. Finally, the product was calcined at 500°C for 4 h and examined by X-ray diffractometry (XRD). The morphology was investigated by SEM and FTIR.

2.1. Modification of CuO-np with 3-(aminopropyl)triethoxysilane

The CuO-np adsorbed water, to remove that CuO-np were kept in an oven at 120°C for 1 d. The dried CuO-np were later sonicated 30 min in 30 mL absolute ethanol, followed by the addition of APTES. The mixture was sonicated again in ice–water for 30 min and then stirred for 24 h. The black product thus obtained was dried at 60°C [33]. The prepared A-CuO-np was later used for the fabrication of the membranes. The surface modification of CuO-np is depicted in Fig. 1.

2.2. Membrane fabrication

At first, the adsorbed water from A-CuO-np was removed by drying at 120°C in an oven for 24 h. The phase inversion method was used to synthesize A-CuO-np integrated CTA membranes. For this purpose, CTA (200 mg) was dissolved in 20 mL of DCM at room temperature. Added 0.3 mL of 2-NPOE in 5 mL of DCM. A solution containing the A-CuO-np was added after vigorous the solution was allowed to stir for half an hour and a homogeneous solution was obtained. Afterwards the DCM was evaporated, and the membrane was dried for the whole night. Later, the formed membrane was detached by immersing in the water for 1 h. The illustration of the membrane fabrication is depicted in Fig. 2.

2.3. Characterization

The fabricated membranes were characterized with EVO-LS 10 (Carl Zeiss, Germany) scanning electron microscope (SEM) and Bruker Vector 22 Fourier transform infrared (FTIR) spectrometer.

2.4. Dye transport experiment

A cell with two detachable glass compartments was employed for performing transport experiments. A pictorial representation of the transport cell is shown in Fig. 3. Between the chambers, the polymer inclusion membrane integrated with CuO (membrane a) and A-CuO-np (membrane b) was placed (in separate experiments), and the compartments were sealed with steel screws. To stop any leakage
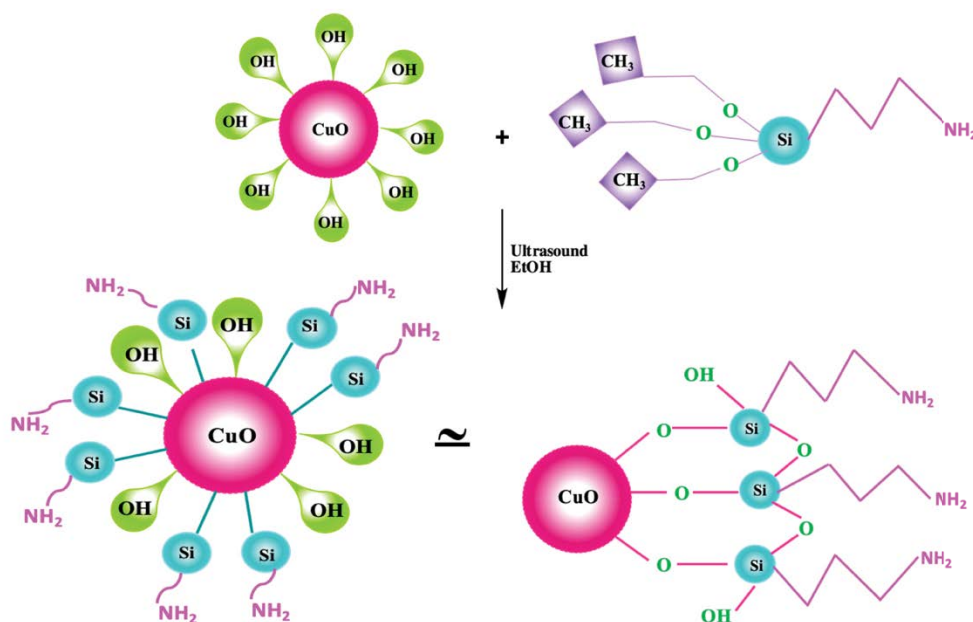

Fig. 1. Surface modification of CuO nanoparticles with 3-(aminopropyl)triethoxysilane.
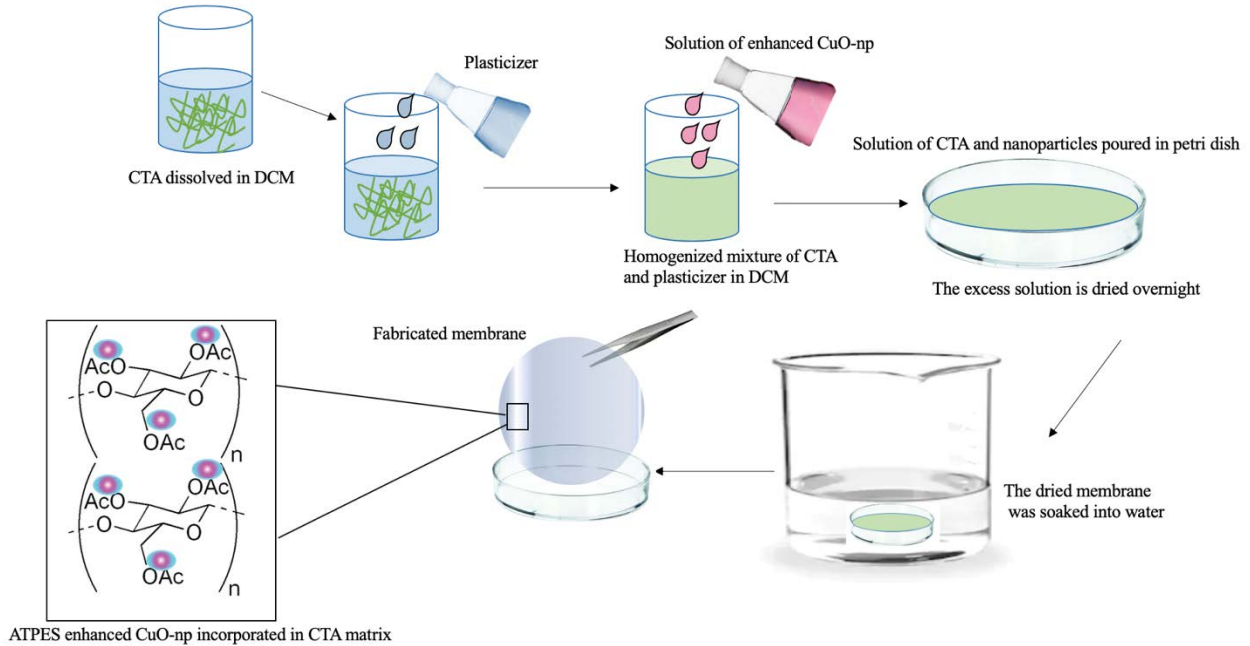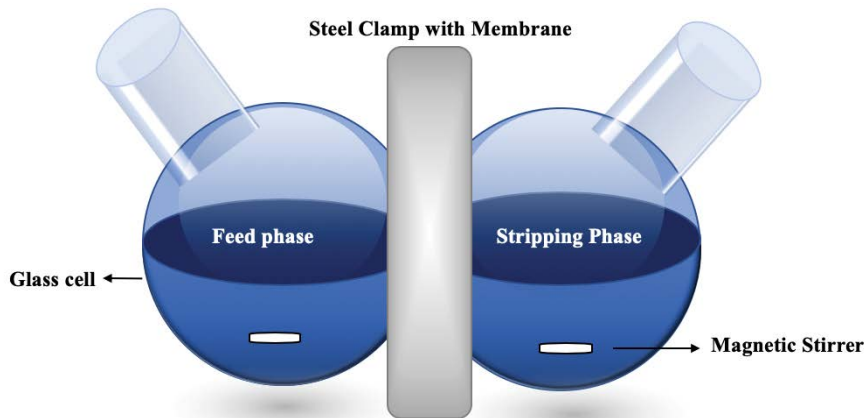
Fig. 2. Process of fabrication of membrane.

Fig. 3. Pictorial representation of glass cell assembly used for transport experiment.

from the chambers the silicone rubber seals were used. One of the chambers was termed a feed chamber and the other was a stripping chamber. Both chambers of the transport cell contained equal volumes (40 mL) of the feed and stripping phase. The stirring is kept constant (300 rpm) in both phases, throughout the experiment. The whole experiment was conducted at 25°C ± 1°C, whereas the effective area of the membrane was 7.0 cm^2 [37]. The investigated experimental factors were MB concentration in feed phase compartment 0.025–0.1 (%w/w), the concentration of strip phase and initial pH (2.0–14.0) and transport time. The transport of MB was found to be in consistency with the following equation.

$$\text{Transport}\,(\%) = 100 \times \left(\frac{C_S}{C_0} \right) \tag{1}$$

where C_S is the concentration of MB in strip phase, at time t where C_0 is MB concentration in the feed phase. For the determination of the concentration of MB, 1 mL of both the phases was drawn at regular intervals and examined by Shimadzu UV-1800, JAPAN UV spectrophotometer.

3. Results and discussion

3.1. FTIR analysis of fabricated membranes

The modification of the CuO nanoparticles with APTES was confirmed by FTIR analysis. The FTIR peak values and the corresponding radicals of various components of membranes are shown in Table 1. The synthesis of CuO is confirmed by the peak at 452 cm^{-1} in the FTIR spectrum because this absorption band is characteristic of the Cu–O

stretching vibrations [38]. The peak values for the pure CuO nanoparticles, the O–H stretch band of the absorbed water carbon dioxide and molecules appear as wide absorption bands centered at 3,480 and 1,635 cm⁻¹. This is due to the high surface area of the nanocrystalline materials. Nanocrystalline substances are usually better than those of traditional polycrystalline-grained substances. These materials depict enhanced strength, diffusivity, ductility, electrical resistivity, specific heat, thermal expansion coefficient, lower thermal conductivity and density [39]. The weak band at 2,950 cm⁻¹ in the FTIR spectrum of the CTA is associated with the aliphatic C–H group's stretch modes. The stretching vibration of the C=O group forms the absorption peak at 1,740 cm⁻¹. While peak at 1,370 cm⁻¹

is due to distortion of C–H in CH₃. C–O stretching vibrations are also confirmed by two peaks around 1,030 and 1,210 cm⁻¹. The well-rounded membrane's peak values in enhanced CuO nanoparticles and the presence of distinctive bands of APTES denote the coupling agent's existence after modification. The CH₂ and CH₃ groups of APTES depict bands at 2,850 and 2,954 cm⁻¹ [19]. The fading of the band around 817 cm⁻¹ is associated with Si–O–CH₃, and the formation of Si–O–Cu bonds is confirmed by the existence of a new peak at 950 cm⁻¹ [40–42]. Hence all these attributes confirm that the grafting of silane molecules on the surface of CuO nanoparticles. The FTIR spectra of the prepared membranes are shown in Fig. 4.

3.2. SEM characterization of fabricated membranes

Surface of the membranes were also characterized with SEM. Fig. 5 depicts the effect of the addition of CuO and A-CuO-np to the membrane surface. The SEM images of the surface of pure membrane (without nanoparticles) appeared to be very smooth in comparison to the other membranes. The presence of the additives is evident in the SEM images as they can be seen as grain like structures in the SEM images. Similar results have been found by Rambabu and Velu [43] whereas "membrane b" was the roughest in appearance as seen by the SEM analysis. The roughness of the formation of clusters or aggregates of CuO and A-CuO nanoparticles on the membrane surface significantly increased with the increase in concentration of the added nanoparticles. Such results were also discovered by Balta et al. [44]. The agglomeration can be attributed to the attraction of CuO by the lone pairs of electrons present on the Oxygen atoms of the CTA matrix [45].

Table 1
FTIR peak values and the corresponding radical in membranes

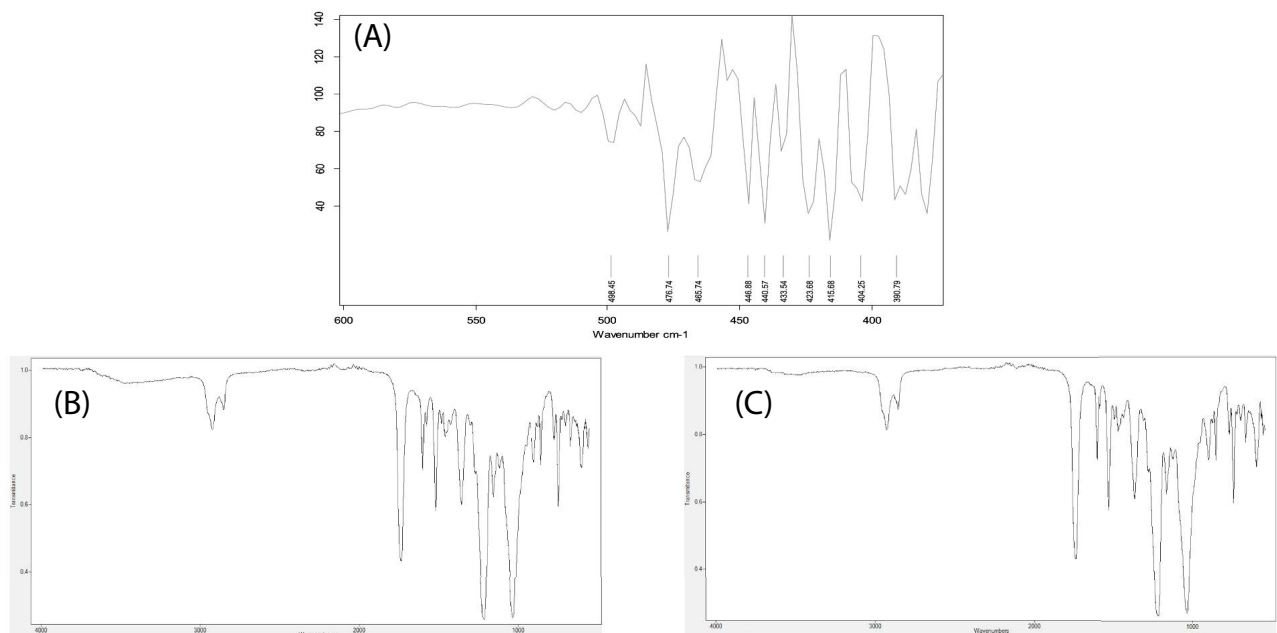| Membrane	Peak value (cm⁻¹)	Corresponding radical
CTA	1,210 and 1,030	C–O
	1,350	C–H (CH₃ deformation)
	1,740	C=O
	2,950	C–H
	3,480	O–H
CuO	1,636 and 3,448	O–H
	452	Cu–O
CTA/ A-CuO-np	All CTA bands	
	817	Si–O–CH₃
	950	Si–O–Cu
	2,850	C–H
	2,975	H–C–NH₂

Fig. 4. FTIR spectra of fabricated membranes: (A) pure membrane, (B) CTA/CuO-np membrane, and (C) CTA/A-CuO-np membrane.
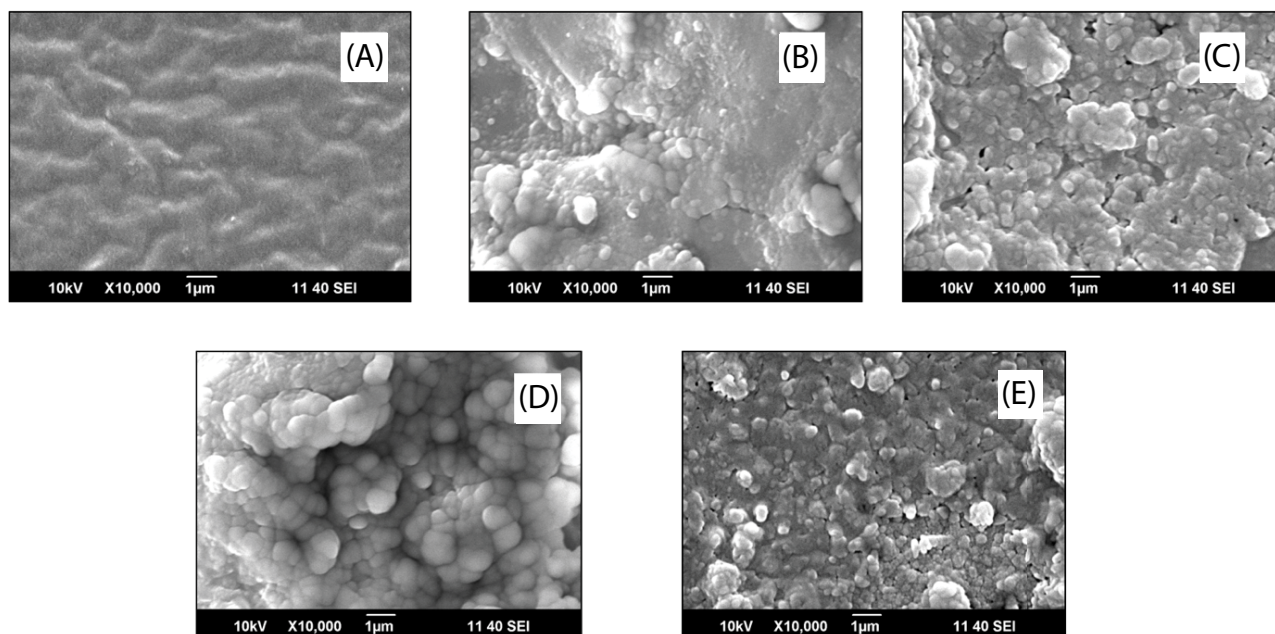
Fig. 5. (A) Pure membrane, (B) 1.0% CTA/CuO-np membrane, (C) 1.0% CTA/A-CuO-np membrane, (D) 2% CTA/CuO-np membrane, and (E) 2.0% CTA/A-CuO-np membrane.

3.3. Transport experiments

The experiment was conducted at varying pH, that is, 4.0, 6.0, 8.0, 10.0 and 12.0 to analyze the impact of feed phase pH on the transportation of MB. An increase in transport of the dye was found in acidic environment. The acidic environment in strip phase makes the dye acidic allowing it simple binding with the basic amino groups of the modified nanoparticles. Similarly, the detaching of the modified nanoparticles and the dye occurs in the strip phase which operates in basic conditions. The pH 4 was used as optimized value as maximum transportation of MB from feed to stripping was achieved as shown in Fig. 6a. The stirring speed of experiment was also optimized in a set of experiments. The high speeds a decrease in transport of the dyes was observed, mainly due to the splashing of the solvent, as this results into the loss of the targeted molecules. At low speed the contact of the nanoparticles and the dye molecules is reduced, resulting into the limited chemical binding of the nanoparticle and the dye leading to the lower transportation. At high speed the splashing causes the loss of the material resulting in the decreased transport between the phases. Maximum transport of the dye was observed at 300 rpm. The results are shown in Fig. 6b. Similar experiments were performed for the optimization of time, at 3 h maximum transportation was observed afterwards the rate of transport became constant (Fig. 6c). The increase in the rate of the transport of the dye with time might be related to the availability of the carriers and dye molecules, with the increasing time the binding of the carrier and dye increased but after certain time (3 h) the carriers become saturated with the dye and a further increase in the time will no longer affect the transportation of the dye. The experiments for optimization of the pH, speed and

were carried out at 0.05% concentration of MB and 1% concentration of the carrier nanoparticles.

The optimized concentration of the carrier and dye was determined at the optimized at pH 4 and 300 rpm. Maximum efficiency was obtained at 1% concentration of the carrier nanoparticles (Fig. 7a). The transport experiments were also performed at the varying concentrations of the dye ranging from of 0.005%–0.1% at optimum pH and room temperature to judge the effect of the MB concentration on its transportation through the nanohybrid membrane. The maximum transportation of the dye was observed at 0.05% concentration of MB by using CTA/A-CuO-np membranes. The results are shown in Fig. 7b. The results of CTA/A-CuO-np membrane in the transport of MB were comparable to CTA/CuO membrane.

The transport of the dye between the phases is driven by the chemical force, the difference in the pH of both the phases allow the nanoparticles to bind with the dye in the feed phase and gets detached from it in the strip phase. The stripping phase interface involves the reaction between the MB-A-CuO-np complex and [OH]⁻ leading to the diffusion of dye into the stripping phase. The proposed mechanism for the functioning of both membranes is shown in Fig. 8 [19]. [OH]⁻ is present in the stripping phase this was to obtain the de-complexing of dye–A-CuO-np complex. The alkaline environment was achieved by the addition of 0.1 M solution of NaOH.

4. Conclusion

In the current study amino enhanced CuO nanoparticles were prepared with 3-(aminopropyl)triethoxysilane (APTES). Later nanohybrid CTA membranes were fabricated via phase inversion enhanced by the CuO-np and A-CuO-np.
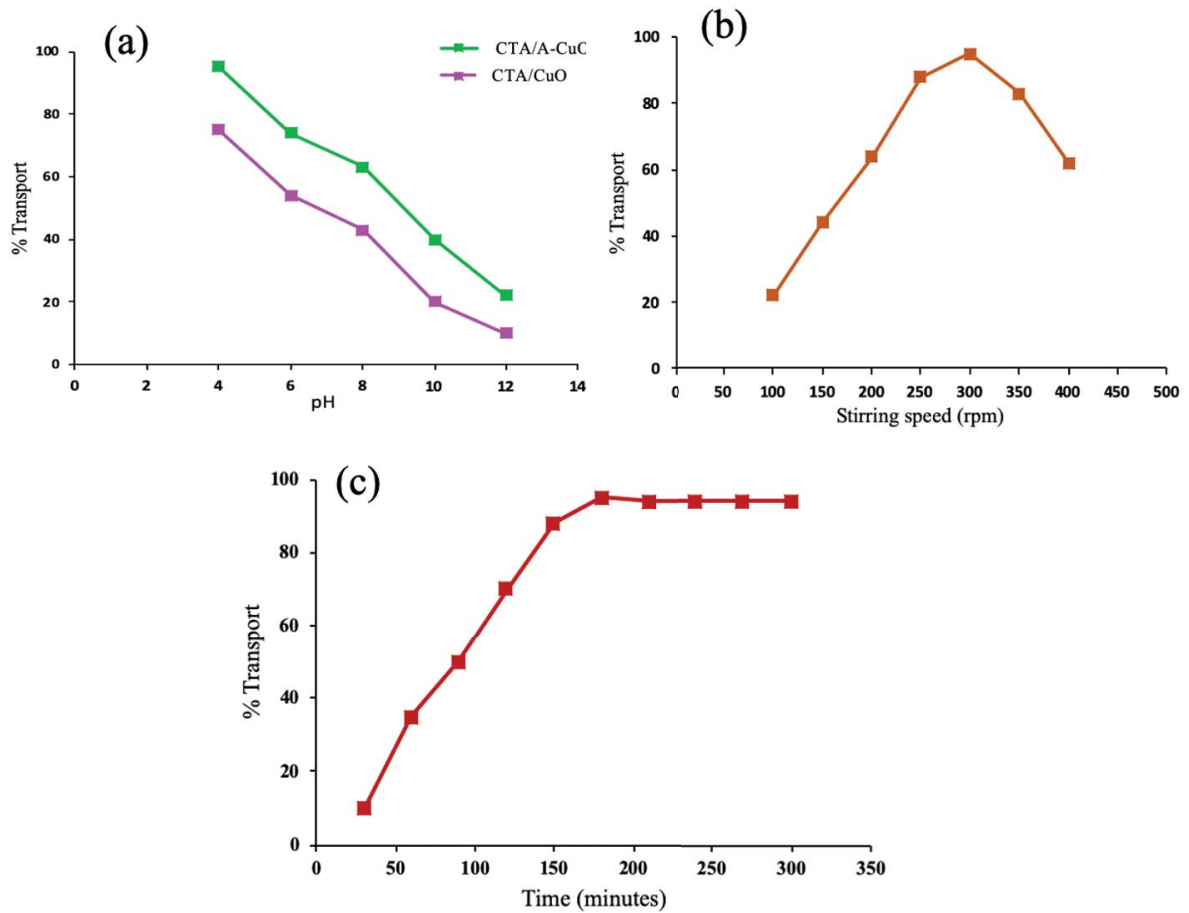
Fig. 6. (a) Effect of pH on % transport of the dye, (b) effect of stirring speed on % transport of the dye, and (c) effect of time on % transport of the dye.
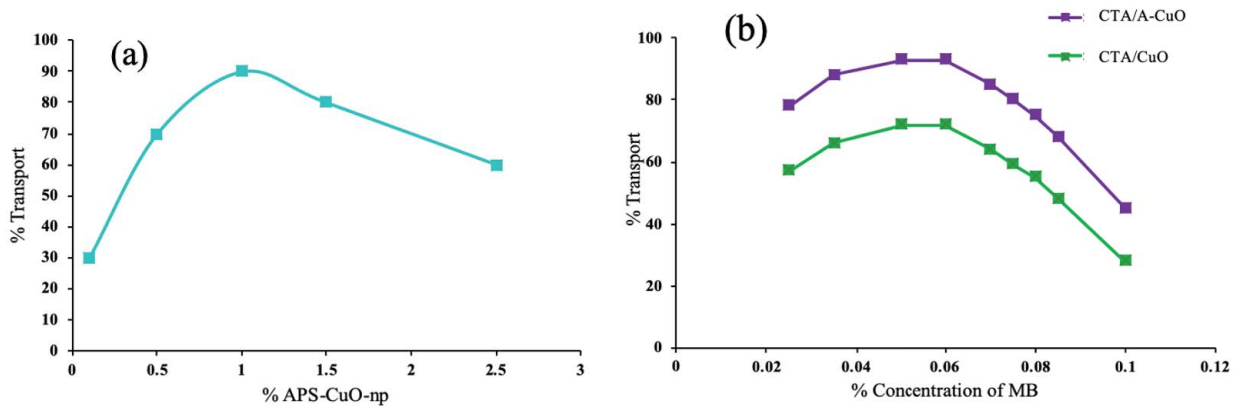

Fig. 7. (a) Effect of the percentage of the carrier in the transport of the dye and (b) effect of percentage concentration of the dye in the transport of dye.

The fabricated membranes were characterized with FTIR and SEM. Afterwards the fabricated membranes were employed for the transport of dye between feed and stripping phase. Different factors like pH of the feed/stripping phase and concentration of the dye were optimized in the later part of the experiment. The membrane modified with the A-CuO showed better transportation of the dyes as compared to the CuO-np modified membranes. This can be associated to the presence of amino groups on A-CuO-np membranes, which offers the better binding of the dye molecules to the
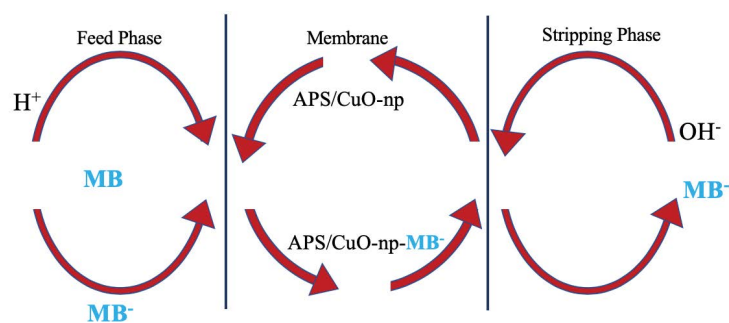
Fig. 8. Proposed mechanism for transport of dye through nanoparticles embedded polymer inclusion membrane.

carrier. It was concluded that CTA/A-CuO-np membrane at 300 rpm, 25°C, 4 pH for feed phase and alkaline stripping phase depicts 97% transport of MB from feed phase to stripping phase. These membranes can be used for the transport of dyes from desirable solvent to the unwanted solvents. After transportation the water can be used again in textile industry. Similarly, the change of the carrier can provide dye selectivity, in that case a particular pigment can be moved from the one phase to another.

Acknowledgement

References

[1] N.H. Al-Shaalan, I. Ali, Z.A. ALOthman, L.H. Al-Wahaibi, H. Alabdulmonem, High performance removal and simulation studies of diuron pesticide in water on MWCNTs, J. Mol. Liq., 289 (2019) 111039, doi: 10.1016/j.molliq.2019.111039.

[2] M.A. Khan, A.A. Alqadami, M. Otero, M.R. Siddiqui, Z.A. ALOthman, I. Alsohaimi, M. Rafatullah, A.E. Hamedelniel, Heteroatom-doped magnetic hydrochar to remove post-transition and transition metals from water: synthesis, characterization, and adsorption studies, Chemosphere, 218 (2019) 1089–1099.

[3] I. Ali, O.M.L. Alharbi, Z.A. Alothman, A. Alwarthan, Facile and eco-friendly synthesis of functionalized iron nanoparticles for cyanazine removal in water, Colloids Surf., B, 171 (2018) 606–613.

[4] Z.A. Alothman, A.Y. Badjah, I. Ali, Facile synthesis and characterization of multi walled carbon nanotubes for fast and effective removal of 4-tert-octylphenol endocrine disruptor in water, J. Mol. Liq., 275 (2019) 41–48.

[5] K. Vijayaraghavan, T.K. Ramanujam, N. Balasubramanian, In situ hypochlorous acid generation for the treatment of textile wastewater, Color. Technol., 117 (2001) 49–53.

[6] S. Patil, S. Renukdas, N. Patel, Removal of methylene blue, a basic dye from aqueous solutions by adsorption using teak tree (*Tectona grandis*) bark powder, Int. J. Environ. Sci., 1 (2011) 711–726.

[7] I. Ali, Z.A. Alothman, A. Alwarthan, Supra molecular mechanism of the removal of 17-β-estradiol endocrine disturbing pollutant from water on functionalized iron nano particles, J. Mol. Liq., 241 (2017) 123–129.

[8] M.A. Khan, A.A. Alqadami, S.M. Wabaidur, M.R. Siddiqui, B.-H. Jeon, S.A. Alshareef, Z.A. Alothman, A.E. Hamedelniel, Oil industry waste based non-magnetic and magnetic hydrochar to sequester potentially toxic post-transition metal ions from water, J. Hazard. Mater., 400 (2020) 123247, doi: 10.1016/j.jhazmat.2020.123247.

[9] M. Gharehbaghi, F. Shemirani, A novel method for dye removal: ionic liquid-based dispersive liquid–liquid extraction (IL-DLLE), Clean–Soil Air Water, 40 (2012) 290–297.

[10] W.-J. Lau, A.F. Ismail, Polymeric nanofiltration membranes for textile dye wastewater treatment: preparation, performance evaluation, transport modelling, and fouling control—a review, Desalination, 245 (2009) 321–348.

[11] F.N. Memon, S. Memon, F.T. Minhas, Rapid transfer of methyl red using calix[6]arene as a carrier in a bulk liquid membrane, C.R. Chim., 17 (2014) 577–585.

[12] T. Poursaberi, M. Hassanisadi, Magnetic removal of reactive Black 5 from wastewater using ionic liquid grafted-magnetic nanoparticles, Clean–Soil Air Water, 41 (2013) 1208–1215.

[13] D. Roy, K.T. Valsaraj, S.A. Kottai, Separation of organic dyes from wastewater by using colloidal gas aphrons, Sep. Sci. Technol., 27 (1992) 573–588.

[14] M. Turabık, B. Gozmen, Removal of basic textile dyes in single and multi-dye solutions by adsorption: statistical optimization and equilibrium isotherm studies, Clean–Soil Air Water, 41 (2013) 1080–1092.

[15] I. Zaharia, I. Diaconu, E. Ruse, G. Nechifor, The transport of 3-aminophenol through bulk liquid membrane in the presence of Aliquat 336, Dig. J. Nanomater. Biostruct., 7 (2012) 1303–1314.

[16] L.D. Nghiem, P. Mornane, I.D. Potter, J.M. Perera, R.W. Cattrall, S.D. Kolev, Extraction and transport of metal ions and small organic compounds using polymer inclusion membranes (PIMs), J. Membr. Sci., 281 (2006) 7–41.

[17] M.I.G.S. Almeida, R.W. Cattrall, S.D. Kolev, Recent trends in extraction and transport of metal ions using polymer inclusion membranes (PIMs), J. Membr. Sci., 415 (2012) 9–23.

[18] D. Kogelnig, A. Regelsberger, A. Stojanovic, F. Jirsa, R. Krachler, B.K. Keppler, A polymer inclusion membrane based on the ionic liquid trihexyl (tetradecyl) phosphonium chloride and PVC for solid–liquid extraction of Zn(II) from hydrochloric acid solution, Monatsh. Chem., 142 (2011) 769–772.

[19] I. Akin, M. Ersoz, Preparation and characterization of CTA/m-ZnO composite membrane for transport of Rhodamine B, Desal. Water Treat., 57 (2016) 3037–3047.

[20] J.S. Gardner, J.O. Walker, J.D. Lamb, Permeability and durability effects of cellulose polymer variation in polymer inclusion membranes, J. Membr. Sci., 229 (2004) 87–93.

[21] N. Pereira, A. St. John, R.W. Cattrall, J.M. Perera, S.D. Kolev, Influence of the composition of polymer inclusion membranes on their homogeneity and flexibility, Desalination, 236 (2009) 327–333.

[22] S.V. Joshi, A.V. Rao, Cellulose triacetate membranes for seawater desalination, Desalination, 51 (1984) 307–312.

[23] R.O. Mazzei, E. Smolko, A. Torres, D. Tadey, C. Rocco, L. Gizzi, S. Strangis, Radiation grafting studies of acrylic acid onto cellulose triacetate membranes, Radiat. Phys. Chem., 64 (2002) 149–160.

[24] I.L. Alsvik, K.R. Zodrow, M. Elimelech, M.-B. Hägg, Polyamide formation on a cellulose triacetate support for osmotic membranes: effect of linking molecules on membrane performance, Desalination, 312 (2013) 2–9.

[25] C.-P. Leo, W.P.C. Lee, A.L. Ahmad, A.W. Mohammad, Polysulfone membranes blended with ZnO nanoparticles for reducing fouling by oleic acid, Sep. Purif. Technol., 89 (2012) 51–56.

[26] R. Bloch, Hydrometallurgical Separations by Solvent Membranes, J.E. Flinn, Ed., Membrane Science and Technology: Industrial, Biological, and Waste Treatment Processes, Springer US, Boston, MA, 1970, pp. 171–187.

[27] E.L. Cussler, R. Aris, A. Bhown, On the limits of facilitated diffusion, J. Membr. Sci., 43 (1989) 149–164.

[28] K.M. White, B.D. Smith, P.J. Duggan, S.L. Sheahan, E.M. Tyndall, Mechanism of facilitated saccharide transport through plasticized cellulose triacetate membranes, J. Membr. Sci., 194 (2001) 165–175.

[29] P. Kallem, G. Bharath, K. Rambabu, C. Srinivasakannan, F. Banat, Improved permeability and antifouling performance of polyethersulfone ultrafiltration membranes tailored by hydroxyapatite/boron nitride nanocomposites, Chemosphere, 268 (2021) 129306, doi: 10.1016/j.chemosphere.2020.129306.

[30] K. Rambabu, G. Bharath, P. Monash, S. Velu, F. Banat, M. Naushad, G. Arthanareeswaran, P.L. Show, Effective treatment of dye polluted wastewater using nanoporous $CaCl_2$ modified polyethersulfone membrane, Process Saf. Environ. Prot., 124 (2019) 266–278.

[31] S. Velu, K. Rambabu, P. Monash, C. Sharma, Improved hydrophilic property of PES/PEG/$MnCO_3$ blended membranes for synthetic dye separation, Int. J. Environ. Sci., 75 (2018) 592–604.

[32] M. Baghbanzadeh, D. Rana, T. Matsuura, C.Q. Lan, Effects of hydrophilic CuO nanoparticles on properties and performance of PVDF VMD membranes, Desalination, 369 (2015) 75–84.

[33] N. Nasrollahi, S. Aber, V. Vatanpour, N.M. Mahmoodi, The effect of amine functionalization of CuO and ZnO nanoparticles used as additives on the morphology and the permeation properties of polyethersulfone ultrafiltration nanocomposite membranes, Compos. B. Eng., 154 (2018) 388–409.

[34] P.H. Krishnamurthy, L.T. Yogarathinam, A. Gangasalam, A.F. Ismail, Influence of copper oxide nanomaterials in a poly (ether sulfone) membrane for improved humic acid and oil–water separation, J. Appl. Polym. Sci., 133 (2016) 43873, doi: 10.1002/app.43873.

[35] N. Nasrollahi, S. Aber, V. Vatanpour, N.M. Mahmoodi, Development of hydrophilic microporous PES ultrafiltration membrane containing CuO nanoparticles with improved antifouling and separation performance, Mater. Chem. Phys., 222 (2019) 338–350.

[36] K. Phiwdang, S. Suphankij, W. Mekprasart, W. Pecharapa, Synthesis of CuO nanoparticles by precipitation method using different precursors, Energy Procedia, 34 (2013) 740–745.

[37] A. Yilmaz, G. Arslan, A. Tor, I. Akin, Selectively facilitated transport of Zn(II) through a novel polymer inclusion membrane containing Cyanex 272 as a carrier reagent, Desalination, 277 (2011) 301–307.

[38] V.A.F. Samson, K.M. Racik, S. Prathap, J. Madhavan, M.V.A. Raj, Investigations of structural, optical and dielectric studies of copper oxide nanoparticles, Mater. Today:. Proc., 8 (2019) 386–392.

[39] C. Suryanarayana, Structure and properties of nanocrystalline materials, Bull. Mater. Sci., 17 (1994) 307–346.

[40] M.S. Mauter, Y. Wang, K.C. Okemgbo, C.O. Osuji, E.P. Giannelis, M. Elimelech, Antifouling ultrafiltration membranes via post-fabrication grafting of biocidal nanomaterials, ACS Appl. Mater. Interfaces, 3 (2011) 2861–2868.

[41] O. Arous, F.S. Saoud, H. Kerdjoudj, Cellulose Triacetate Properties and Their Effect on the Thin Films Morphology and Performance, IOP Conference Series Materials Science and Engineering, 12 (2010) 012001, doi: 10.1088/1757-899X/12/1/012001.

[42] R.-P. Ye, L. Lin, C.-C. Chen, J.-X. Yang, F. Li, X. Zhang, D.-J. Li, Y.-Y. Qin, Z. Zhou, Y.-G. Yao, Synthesis of robust MOF-derived Cu/SiO_2 catalyst with low copper loading via sol–gel method for the dimethyl oxalate hydrogenation reaction, ACS Catal., 8 (2018) 3382–3394.

[43] K. Rambabu, S. Velu, Improved performance of $CaCl_2$ incorporated polyethersulfone ultrafiltration membranes, Period. Polytech., Chem. Eng., 60 (2016) 181–191.

[44] S. Balta, A. Sotto, P. Luis, L. Benea, B. Van der Bruggen, J. Kim, A new outlook on membrane enhancement with nanoparticles: the alternative of ZnO, J. Membr. Sci., 389 (2012) 155–161.

[45] R. Krishnamoorthy, V. Sagadevan, Polyethylene glycol and iron oxide nanoparticles blended polyethersulfone ultrafiltration membrane for enhanced performance in dye removal studies, e-Polymers, 15 (2015) 151–159.